J. Biochem. 126, 668-675 (1999)

Unusually High Standard Redox Potential of Acrylyl-CoA/Propionyl-CoA Couple among Enoyl-CoA/Acyl-CoA Couples: A Reason for the Distinct Metabolic Pathway of Propionyl-CoA from Longer Acyl-CoAs

Kyosuke Sato,*[,1] Yasuzo Nishina,* Chiaki Setoyama,† Retsu Miura,† and Kiyoshi Shiga*

*Departments of *Physiology and †Biochemistry, Kumamoto University School of Medicine, Honjo 2-2-1, Kumamoto 860-0811*

Received June 24, 1999; accepted July 14, 1999

The standard redox potential of acrylyl-CoA/propionyl-CoA couple (C_3) was determined to be 69 mV (*vs.* standard hydrogen electrode) at pH 7 and 25°C. This value implies that the 2,3-dehydrogenation of propionyl-CoA is thermodynamically much more unfavorable than that of longer acyl-CoAs because the standard redox potentials of crotonyl-CoA/butyryl-CoA (C_4), octenoyl-CoA/octanoyl-CoA (C_8), and hexadecenoyl-CoA/palmitoyl-CoA (C_{16}) are all about −10 mV. The unusually high standard redox potential of the acrylyl-CoA/propionyl-CoA couple is thought to be one of the reasons that in mammals propionyl-CoA is not metabolized by β-oxidation as in the case of longer acyl-CoAs, but by a methylmalonyl-CoA pathway. The obvious structural difference between C_3 and C_4 (and longer) is whether an H or the C(4) atom is connected to -C(3)H=C(2)H-C(1)O-S-CoA. The molecular orbital calculations (MOPAC) for the enoyl and acyl forms of C_3 and C_4 revealed that this structural feature is the main cause for the higher standard redox potential of the C_3 couple. That is, the C(4)-C(3) bond is stabilized by the dehydrogenation to a greater degree than the H-C(3) bond.

Key words: acrylyl-CoA, acyl-CoA dehydrogenase, propionate oxidation, propionyl-CoA, standard redox potential.

In mitochondria, straight chain fatty acids are metabolized in their CoA thioester forms by a β-oxidation cycle (*1, 2*). An acyl-CoA with an acyl chain length of n (C_n) is converted by β-oxidation to an acyl-CoA with a chain length shorter by two (C_{n-2}) plus acetyl-CoA (C_2). One cycle of β-oxidation includes four steps. The first step is the desaturation of the acyl-CoA to its 2-*trans*-enoyl-CoA form.

$$R\text{-}CH_2\text{-}CH_2\text{-}CO\text{-}S\text{-}CoA \longrightarrow R\text{-}CH{=}CH\text{-}CO\text{-}S\text{-}CoA + 2H$$

This reaction is catalyzed by four kinds of acyl-CoA dehydrogenases that differ in their specificities for substrates with various chain lengths: very long-chain, long-chain, medium-chain, and short-chain acyl-CoA dehydrogenases (*1*).

Propionyl-CoA is an acyl-CoA with a chain length of three (C_3). Propionyl-CoA is formed by the β-oxidation of odd-numbered or methyl-branched acyl-CoAs and by the degradation of amino acids such as valine, isoleucine, threonine, and methionine (*2*). In addition, propionate is produced by ruminal bacteria and is one of the major carbon sources for ruminants (*2*). In mammals, propionate or propionyl-CoA metabolism differs from the β-oxidation of longer fatty acids. The main metabolic pathway of propionate or propionyl-CoA is the methylmalonyl-CoA pathway to form succinate (*2, 3*).

Propionyl-CoA ($CH_3\text{-}CH_2\text{-}CO\text{-}S\text{-}CoA$) can be oxidized to acrylyl-CoA ($CH_2{=}CH\text{-}CO\text{-}S\text{-}CoA$) by short-chain acyl-CoA dehydrogenase, but the reaction is much slower (0.3%) than that involving butyryl-CoA (*4*). This may be a reason for that for the most part mammals do not metabolize propionyl-CoA by β-oxidation.

This paper concerns the physicochemical nature of enoyl-CoA/acyl-CoA couples. Standard redox potential is one of the most important properties of redox chemicals. The standard redox potential of enoyl-CoA/acyl-CoA couples was first determined by Hauge (*5*) for crotonyl-CoA/butyryl-CoA (C_4) as −15 mV (pH 7, 30°C). More recently, Stankovich and Soltysik (*6*) redetermined it as −13 mV (pH 7, 15°C). Further, Lenn *et al.* (*7*) measured the standard redox potentials of enoyl-CoA/acyl-CoA couples of different chain lengths: at pH 7.6 and 25°C, −45 mV for crotonyl-CoA/butyryl-CoA (C_4), −41 mV for octenoyl-CoA/octanoyl-CoA (C_8), and −38 mV for hexadecenoyl-CoA/palmitoyl-CoA (C_{16}); the corrected values for pH 7 are −10 (C_4), −6 (C_8), and −3 mV (C_{16}). These results can be summarized as indicating that the standard redox potentials of enoyl-CoA/acyl-CoA couples with chain lengths from C_4 to C_{16} are all nearly the same with values near −10 mV. Somewhat surprisingly, however, the value for acrylyl-CoA/propionyl-CoA (C_3) has not been reported to our knowledge. In order to understand the unique

[1] To whom correspondence should be addressed.

Abbreviations: C_n, acyl-CoA or enoyl-CoA with n carbon atoms in the acyl or enoyl group; CoA, coenzyme A; HOF, heat of formation.

metabolism of propionyl-CoA described above, it is important to evaluate the redox property of the C_3 couple. In this study, we found that the standard redox potential of the C_3 couple is unusually high compared with those with longer chain lengths. This is one of the reasons that acyl-CoA dehydrogenase does not oxidize propionyl-CoA efficiently. Further, we discuss the reason for this extraordinary redox feature of the C_3 couple.

MATERIALS AND METHODS

Reagents—CoA-SH was purchased from Kojin and acryloyl chloride was from Aldrich. All other chemicals were obtained from Nacalai Tesque.

Instruments—A Hitachi U-3210 spectrophotometer was used for spectrophotometric measurements. The HPLC system comprised an L-6200 intelligent pump (Hitachi) and an MCPD-3600 spectro multi channel photo detector (Otsuka Electronics). Oxidation-reduction potential was measured with a HORIBA 6860-10C combined platinum/Ag-AgCl electrode connected to a HORIBA M-8s pH meter. The electrode potential was calibrated using a solution of 6 mg/ml quinhydrone in 50 mM potassium phosphate (pH 7) at 25°C (286 mV *vs.* a standard hydrogen electrode) as described (*8*).

Coenzyme A Thioesters—Acrylyl-CoA was synthesized by the acid chloride method (*9*). Propionyl-CoA, butyryl-CoA, and crotonyl-CoA were synthesized by the acid anhydride method (*10*), but the solvent water was replaced by a water-tetrahydrofuran mixture (1:1 v/v) to solubilize the anhydrides. Pentanoyl-CoA and hexanoyl-CoA were synthesized by the mixed acid anhydride method (*11*). The synthesized CoA thioesters were concentrated with a rotary evaporator and purified by C-18 reversed-phase HPLC with a gradient of 10 mM potassium phosphate buffer (pH 5.3)-methanol. Purified CoA thioesters were concentrated with an evaporator and desalted by gel filtration through Sephadex G-10 (Amersham Pharmacia Biotech) using water as the mobile phase. The concentrated samples were stored frozen at −18°C. Analytical reversed-phase HPLC showed that the CoA thioesters prepared and stored as above were sufficiently pure and stable for at least several months. The concentrations were spectrophotometrically determined using extinction coefficients $\varepsilon_{260} = 16.4\ mM^{-1} \cdot cm^{-1}$ for acyl-CoAs (propionyl-, butyryl-, pentanoyl-, and hexanoyl-CoAs) and $\varepsilon_{260} = 22.6\ mM^{-1} \cdot cm^{-1}$ for enoyl-CoAs (acrylyl-, crotonyl-, pentenoyl-, and hexenoyl-CoAs) (*10*).

Butyryl-CoA Dehydrogenase—The anaerobic bacterium *Megasphaera elsdenii* (JCM 1772) was obtained from the Japan Collection of Microorganisms (the Institute of Physical and Chemical Research, Saitama). The bacteria were grown and the green form of butyryl-CoA dehydrogenase (CoA persulfide-binding form Ref. *12*) was isolated as described previously (*13*). This preparation contains a significant level of crotonase contamination (*14*) that was removed by hydrophobic chromatography as reported (*15*) with the following modification. The green butyryl-CoA dehydrogenase solution in 0.1 M potassium phosphate buffer, pH 6, was taken to 50% saturation with ammonium sulfate and applied to an octyl-Sepharose 4B (Amersham Pharmacia Biotech) column (1.4×22 cm) equilibrated with the same buffer. The tightly adsorbed enzyme at the top of the column was eluted by a linear gradient formed from 200 ml equilibration buffer and 200 ml of 0.1 M potassium phosphate buffer, pH 6. Fractions of 10-ml were collected and assayed for crotonase activity as reported (*15*). A sharp peak of crotonase activity was observed after the peak of green butyryl-CoA dehydrogenase. The purified dehydrogenase was stored as a suspension in 75% ammonium sulfate at 4°C. The CoA-free dehydrogenase was prepared by the reported method (*16, 17*) and stored frozen (−18°C) in 50 mM potassium phosphate buffer, pH 6, containing 20% v/v glycerol. The concentration of the CoA-free butyryl-CoA dehydrogenase was determined spectrophotometrically using an extinction coefficient of $\varepsilon_{450} = 14.4\ mM^{-1} \cdot cm^{-1}$ (*18*).

Anaerobic Experiments—Highly purified argon gas (O_2 content less than 0.2 ppm) purchased from Nippon Sanso was supplied by a low-leakage-type pressure regulator through stainless steel tubing (1/8 inch diameter). A glassware bubbler containing 20 ml water was inserted in the gas line to moisten the gas. A glass tube (5 cm length and 8 mm diameter), the end of which was processed in the shape of the syringe fitting (male), was connected to the end of the stainless tubing. For metal-to-metal joints, a compression-type fitting was used. For metal-to-glass joints, a similar fitting but with an internal silicone O-ring to seal the glass-metal interface, was used.

For anaerobic spectrophotometry, a 50-μl microcell (1-cm light path, 12.5×12.5×50-mm outer size) with a screw cap with a silicone septum on the top was used. Two syringe needles with syringe fittings (female) were made to pierce the silicone septum. One of the syringe needles, made wholly of metal, was fitted to the syringe-fitting-shaped glass end of the gas line. The other syringe needle was the gas outlet and was also the path through which reagents were added using a Hamilton gas-tight microsyringe. Anaerobiosis was achieved by passing a stream of Ar gas at a constant 10 ml/min through the inner space of the cell. The sample solution (about 100 μl) in the cell was agitated by tapping the cell every 5 min to facilitate deoxygenation. Satisfactory anaerobiosis was achieved after 30-60 min, as judged from the deoxygenation of a solution of flavin adenine dinucleotide followed by spectrophotometric titration with sodium dithionite (*19, 20*).

Anaerobiosis of titrants and reaction mixtures that did not require spectrophotometric measurements was achieved in a glass microvial (capacity 0.3 ml) with a screw cap containing a silicone septum through which two syringe needles were inserted.

Measurement of Standard Redox Potential of Acrylyl-CoA/Propionyl-CoA Couples Using a Redox Indicator Dye—The relationship between the redox potential and the absorbance of phenazine ethosulfate was determined using an anaerobic spectrophotometric cell equipped with an oxidation-reduction potential electrode similar to that illustrated previously [Fig. 2 in Cammack's article (*8*) or Fig. 4A in Dutton's paper (*21*)]. This cell allows the simultaneous measurement of redox potential and absorbance. [However, it has the disadvantage of requiring a large volume of sample (7 ml). For this reason we did not measure the redox potential of the solution of acrylyl-CoA and propionyl-CoA directly.] A 7-ml solution of 20 μM phenazine ethosulfate and 1 μM butyryl-CoA dehydrogenase in 50 mM potassium phosphate buffer (pH 7) at 25°C

was deoxygenated under a stream of Ar gas in the cell. Then the dye was reductively titrated with 30 mM butyryl-CoA. The redox potential and the absorbance at 387 nm both became constant within 15 min after each addition of butyryl-CoA; each pair of values was plotted on a graph (inset of Fig. 1, open circles). After the phenazine ethosulfate was almost completely reduced, the dye was gradually reoxidized by introducing air into the cell, and pairs of values (absorbance and redox potential) at several time points were plotted (inset of Fig. 1, closed circles). The absorbance is represented in the ordinate of the inset of Fig. 1 as the relative value compared to the initial absorbance (0.47) before reduction.

To measure the redox potential of a solution of acrylyl-CoA and propionyl-CoA at a given concentration ratio, it is necessary to equilibrate the acrylyl-CoA/propionyl-CoA with phenazine ethosulfate. The reaction between phenazine ethosulfate and the acrylyl-CoA/propionyl-CoA couple is very slow even in the presence of butyryl-CoA dehydrogenase. In order to reduce the time needed to reach equilibrium, the dye was partially reduced with butyryl-CoA in the presence of butyryl-CoA dehydrogenase before the addition of acrylyl-CoA/propionyl-CoA so that the redox state of the dye was near the equilibrium of acrylyl-CoA/propionyl-CoA. The detailed procedure is as follows.

A 100-μl solution of 20 μM phenazine ethosulfate and 1 μM butyryl-CoA dehydrogenase in 50 mM potassium phosphate buffer (pH 7) was deoxygenated in the anaerobic 50 μl-microcell. Then a small volume (less than 4 μl) of an anaerobic solution of 500 μM butyryl-CoA was added to partially reduce the dye. The absorbance at 387 nm decreased gradually. After the absorbance reached a constant value (10-30 min), an anaerobic solution (2 μl) of a mixture of acrylyl-CoA and propionyl-CoA (total 10 mM) was added to give a final total concentration of 200 μM. The absorbance at 387 nm was monitored continuously. If the absorbance did not reach a constant value within 60 min, the reaction was attempted again using a different amount of butyryl-CoA. The redox potential at equilibrium was determined from the absorbance (corrected for dilution and divided by the initial absorbance before the addition of butyryl-CoA) using the absorbance-redox potential relationship (inset of Fig. 1).

Reaction of Acrylyl-CoA and Butyryl-CoA—A solution (200 μl) of acrylyl-CoA and butyryl-CoA (both about 100 μM) in 50 mM potassium phosphate buffer (pH 7) was deoxygenated in a glass microvial. The reaction was started by adding deoxygenated butyryl-CoA dehydrogenase (2 μl$\times$100 μM) to a final concentration of 1 μM. At various times, 20-μl aliquots of the reaction mixture were withdrawn and mixed anaerobically with 20 mg solid guanidine hydrochloride to stop the reaction. The protein was removed by ultrafiltration through a Microcon-10 membrane (Amicon), and 20 μl of the filtrate was subjected to C-18 reversed-phase HPLC analysis using a Cosmosil 5C_{18}-MS column (1$\times$25 cm, Nacalai Tesque) with a linearly increasing methanol gradient from 10 mM potassium phosphate buffer, pH 5.3.

MOPAC Calculation—The semi-empirical molecular orbital calculation was carried out using WinMOPAC version 1.0 (Fujitsu) running on Microsoft Windows 95. The keyword line of the MOPAC input file was written as "PM3 ENPART," which provides calculation by the PM3 method and the output of the energy partition.

RESULTS

In this study, we used butyryl-CoA dehydrogenase isolated from the anaerobic bacterium *Megasphaera elsdenii*. This enzyme is similar to the mammalian short-chain acyl-CoA dehydrogenase in many of its properties and has the advantage of being prepared easily in large scale. Butyryl-CoA dehydrogenase is named for its best substrate, butyryl-CoA, but it also dehydrogenates other short-chain acyl-CoAs including propionyl-CoA (*18*).

The standard redox potential of the acrylyl-CoA/propionyl-CoA (C_3) couple was determined using phenazine ethosulfate [$E^{\prime\prime}$=55 mV (*22*)] as a redox indicator. The reaction between phenazine ethosulfate and a mixture of acrylyl-CoA and propionyl-CoA at a given concentration ratio was coupled by butyryl-CoA dehydrogenase. The redox potential at the equilibrium was determined from the absorbance of phenazine ethosulfate at 387 nm using the absorbance-redox potential relationship determined in advance (inset of Fig. 1). In these experiments, the absorbance at 387 nm includes some contribution of butyryl-CoA dehydrogenase, which shows absorbance at 387 nm due to its tightly bound coenzyme, flavin adenine dinucleotide. However, the contribution of the enzyme absorption causes little error in determining the redox potential for the following reasons. (i) The concentrations of phenazine ethosulfate and butyryl-CoA dehydrogenase used in all experiments were constant (20 and 1 μM, respectively). (ii) The absorbance at 387 nm of 1 μM butyryl-CoA dehydrogenase can vary by at most 0.01 depending on the redox potential and ligand binding (*6, 17*). This may cause an error in the determination of the redox potential, but the error would be very small; a difference in absorbance of

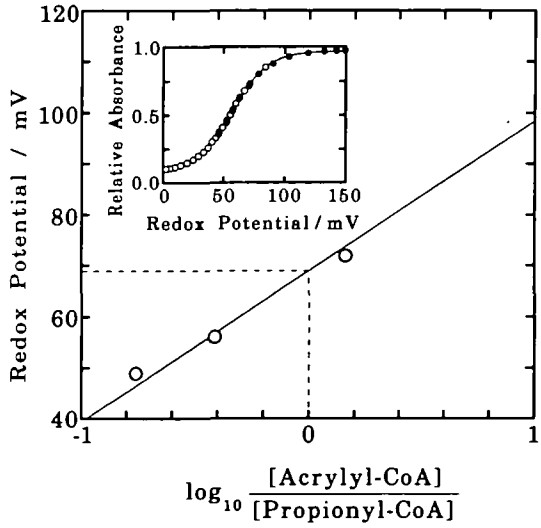

Fig. 1. **Nernst plot for the acrylyl-CoA/propionyl-CoA couple.** A mixture of acrylyl-CoA and propionyl-CoA (total 200 μM) of given concentration ratio was anaerobically equilibrated with 20 μM phenazine ethosulfate in the presence of 1 μM butyryl-CoA dehydrogenase in 50 mM potassium phosphate buffer (pH 7) at 25°C. The inset shows the relationship between the redox potential and the absorbance at 387 nm of phenazine ethosulfate. See "MATERIALS AND METHODS" for details.

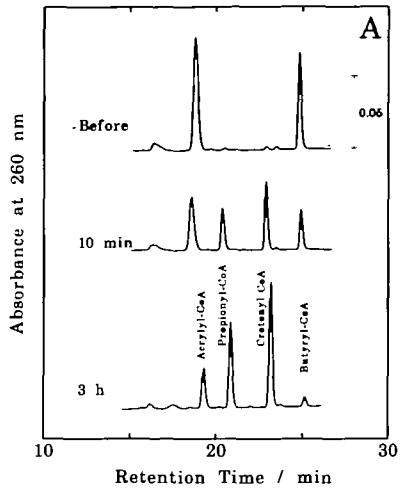

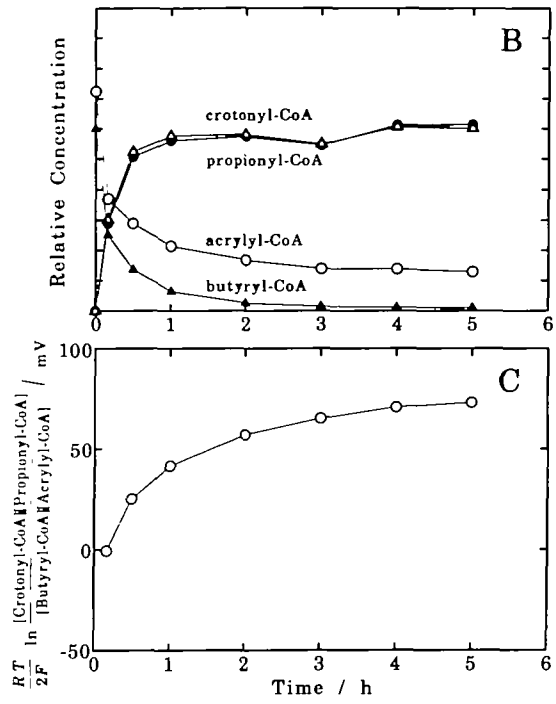

Fig. 2. **Reaction between butyryl-CoA and acrylyl-CoA in the presence of butyryl-CoA dehydrogenase.** Acrylyl-CoA (120 μM) and butyryl-CoA (100 μM) were anaerobically incubated in the presence of butyryl-CoA dehydrogenase (1 μM) at 25°C in 50 mM potassium phosphate buffer, pH 7. Panel A shows the C_{18} HPLC chromatogram of the reaction mixture treated with guanidine hydrochloride at the indicated times after the start of the reaction. The peaks were assigned by comparing the peak positions with those of authentic CoA thioesters. The bar at the top right indicates the absorbance scale. Panel B shows the time course of the reaction. The relative concentrations of the four CoA thioesters at each time were determined by (peak area of absorbance at 260 nm)/ε_{260}. Panel C shows the time course of the value indicated on the ordinate.

0.01, which corresponds to a relative absorbance (ordinate of the inset of Fig. 1) of 0.022, causes a difference in redox potential of less than 1.4 mV according to the absorbance-redox potential relationship shown in the inset of Fig. 1. Figure 1 (main panel) is the Nernst plot for the acrylyl-CoA/propionyl-CoA couple. The standard redox potential was determined to be 69 mV by fitting the data to the Nernst equation,

$$E' = E_3^{\circ\prime} + \frac{RT}{2F} \ln \frac{[\text{acrylyl-CoA}]}{[\text{propionyl-CoA}]},$$

where E' is the redox potential of the redox system, $E_3^{\circ\prime}$ the standard redox potential of the acrylyl-CoA/propionyl-CoA couple, R the gas constant, T the absolute temperature, and F the Faraday constant. The brackets represent molar concentrations. The numeral 2 in the denominator is the number of electrons participating in the reaction.

The standard redox potential of 69 mV for the C_3 couple determined as above is much higher than that of the C_4 couple (about -10 mV, see the "Introduction"). To confirm the large difference in the standard redox potential between the C_3 and C_4 couples, the reaction

$$\text{acrylyl-CoA} + \text{butyryl-CoA} \rightleftharpoons \text{propionyl-CoA} + \text{crotonyl-CoA} \quad (1)$$

was carried out in the presence of butyryl-CoA dehydrogenase. At the equilibrium of reaction 1, the redox potentials of the C_4 and C_3 couples are the same so that

$$E_3^{\circ\prime} + \frac{RT}{2F} \ln \frac{[\text{acrylyl-CoA}]}{[\text{propionyl-CoA}]} = E_4^{\circ\prime} + \frac{RT}{2F} \ln \frac{[\text{crotonyl-CoA}]}{[\text{butyryl-CoA}]},$$

where $E_4^{\circ\prime}$ is the standard redox potential of the C_4 couple. This equation becomes,

$$E_3^{\circ\prime} - E_4^{\circ\prime} = \frac{RT}{2F} \ln \frac{[\text{crotonyl-CoA}][\text{propionyl-CoA}]}{[\text{butyryl-CoA}][\text{acrylyl-CoA}]}, \quad (2)$$

which relates the difference in the standard redox potential between C_3 and C_4 to the proportions of CoA thioester concentrations at equilibrium.

The anaerobic reaction of acrylyl-CoA and butyryl-CoA in the presence of butyryl-CoA dehydrogenase was followed by C-18 reverse-phase chromatography as shown in Fig. 2A. Figure 2B shows the time course of the reaction. The rightward reaction in Eq. 1 proceeds almost completely, indicating that the C_3 couple thermodynamically favors the reduced form (acyl-CoA) much more than the C_4 couple, that is, the standard redox potential of the C_3 couple is much higher than that of the C_4 couple. Figure 2C shows the time course of the value of the right side of Eq. 2, which should coincide at equilibrium with the difference in the standard redox potentials ($E_3^{\circ\prime} - E_4^{\circ\prime}$). The data in Fig. 2C show that the standard redox potential of the C_3 couple is higher by about 80 mV than that of the C_4 couple ($E_3^{\circ\prime} - E_4^{\circ\prime} \simeq 80$ mV). This result is in good agreement with the above result, $E_3^{\circ\prime} = 69$ mV, and the reported result, $E_4^{\circ\prime} \simeq -10$ mV.

The standard redox potentials were also compared among C_4, C_5, and C_6 couples by a similar method as above. The reaction among crotonyl-CoA, pentanoyl-CoA, and hexanoyl-CoA in the presence of butyryl-CoA dehydrogenase was carried out. At equilibrium, the following equations hold.

$$E_5^{\circ\prime} - E_4^{\circ\prime} = \frac{RT}{2F} \ln \frac{[\text{crotonyl-CoA}][\text{pentanoyl-CoA}]}{[\text{butyryl-CoA}][\text{pentenoyl-CoA}]} \quad (3)$$

$$E_6^{\circ\prime} - E_4^{\circ\prime} = \frac{RT}{2F} \ln \frac{[\text{crotonyl-CoA}][\text{hexanoyl-CoA}]}{[\text{butyryl-CoA}][\text{hexenoyl-CoA}]}, \quad (4)$$

where $E_5^{\circ\prime}$ and $E_6^{\circ\prime}$ are the standard redox potentials of the C_5 and C_6 couples. Figure 3 shows the time course of the values of the right side of Eqs. 3 and 4. The values at equilibrium are almost zero within the range of error ($E_5^{\circ\prime} - E_4^{\circ\prime} = 3$ mV and $E_6^{\circ\prime} - E_4^{\circ\prime} = -3$ mV). Thus the standard redox potentials are almost constant among the C_4, C_5, and

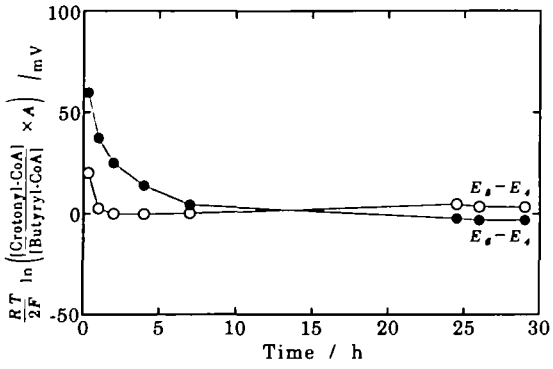

Fig. 3. **Equilibration among the redox couples, crotonyl-CoA/butyryl-CoA, pentenoyl-CoA/pentanoyl-CoA, and hexenoyl-CoA/hexanoyl-CoA.** Crotonyl-CoA (100 μM), pentanoyl-CoA (100 μM), and hexanoyl-CoA (100 μM) were anaerobically incubated in the presence of butyryl-CoA dehydrogenase (1 μM) in 50 mM potassium phosphate buffer, pH 7, at 25°C. The concentrations of the reactants (the three CoA thioesters described above) and products (butyryl-CoA, pentenoyl-CoA, and hexenoyl-CoA) were determined at several times by C_{18} HPLC. The figure shows the values calculated from the concentrations of thioesters as indicated, where A is [pentanoyl-CoA]/[pentenoyl-CoA] (○) or [hexanoyl-CoA]/[hexenoyl-CoA] (●).

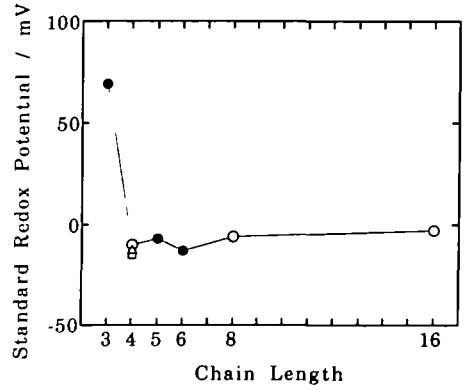

Fig. 4. **Dependence of the standard redox potential of the enoyl-CoA/acyl-CoA couple on chain length.** The open circles show the data of Lenn *et al.* (*7*), the triangle shows that of Stankovich and Soltysik (*6*), and the square shows that of Hauge (*5*). The closed circles are the present results. The value for C_3 was determined from Fig. 1. The values for C_5 and C_6 were determined from Fig. 3 and the value for C_4 shown by the open circle.

C_6 couples.

It has been reported that butyryl-CoA dehydrogenase has an intrinsic enoyl-CoA hydratase activity (*6, 14*). However, the hydratase activity is very weak so that the hydration of enoyl-CoAs is negligible at low enzyme concentrations (*6*). In addition, the presence of acyl-CoAs inhibits the enoyl-CoA hydratase activity of butyryl-CoA dehydrogenase (*6*), probably due to occupation of the active site by acyl-CoAs. In fact, no significant amounts of hydration products (3-hydroxyacyl-CoAs) were detected on the C18 chromatogram in the above experiments, supporting the notion that the intrinsic hydratase activity of butyryl-CoA dehydrogenase does not affect the above results.

Figure 4 summarizes the present results together with the previously reported standard redox potentials for couples of various chain lengths. The results show that the standard redox potential of the C_3 couple is distinctively higher than those of the others.

DISCUSSION

Physiology—Mammalian short-chain acyl-CoA dehydrogenases show optimal activity with butyryl-CoA (C_4) or pentanoyl-CoA (C_5), and less activity with shorter or longer acyl-CoAs. The mechanism for the dependence of activity on chain length has been one of the main subjects of biochemical research on β-oxidation systems. The relative activities of short-chain acyl-CoA dehydrogenases have been reported as C_3:C_4:C_5:C_6:C_7:C_8 = 0.3:100:135:57:10:4 (V_{max}; ox liver enzyme) by Shaw and Engel (*4*) and C_3:C_4:C_5:C_6:C_8 = 0:100:91:13:0 (fixed substrate concentration; rat liver enzyme) by Ikeda *et al.* (*23*). Butyryl-CoA dehydrogenase from *Megasphaera elsdenii* also shows similar substrate specificities: C_3:C_4:C_5:C_6:C_7 = 0.5:100:45:4:0 (V_{max}) (*18*). These data show a gradual decrease in activity upon elongation of the acyl chain from the optimum chain length (C_4 or C_5), but there is a large breakdown upon shortening the acyl chain length from C_4 to C_3. One reasonable and acceptable explanation for the dependence of the activity on chain length is that the interaction between the substrate and the enzyme, or the configuration of the substrate at the active site of the enzyme, is changed by the steric effect of the alkyl chain. However, the drastic difference in activity between C_3 and C_4 does not seem to be ascribed only to the steric factor. In this paper, we demonstrate that the standard redox potential of the acrylyl-CoA/propionyl-CoA couple (C_3) is 69 mV, which is unusually higher than for enoyl-CoA/acyl-CoA couples with longer chains (about −10 mV). That is, the oxidation of propionyl-CoA is thermodynamically more unfavorable than the oxidations of longer acyl-CoAs. This fact can explain the extremely low activity of acyl-CoA dehydrogenases toward propionyl-CoA.

Propionyl-CoA dehydrogenase activity has been described in many microorganisms such as *Salmonella typhimurium* (*24, 25*), *Escherichia coli* (*26, 27*), *Prototheca zopfii* (*28*), and *Moraxella lwoffi* (*29, 30*). For these organisms, however, the dehydrogenase activity was demonstrated only in cell-free extracts. That is, propionyl-CoA dehydrogenases from these organisms have neither been isolated nor characterized at the molecular level. From the data presented in papers of studies using cell-free extracts, the propionyl-CoA dehydrogenase activity in the extract can be estimated to be 3.8 nmol/min/mg protein for *Salmonella typhimurium* (*24*) and 2.5 nmol/min/mg protein for *Prototheca zopfii* (*28*). On the other hand, purified mammalian short-chain acyl-CoA dehydrogenases show a propionyl-CoA dehydrogenase activity of 45 nmol/min/mg enzyme (*31*), while purified *Megasphaera elsdenii* butyryl-CoA dehydrogenase shows an activity of 40 nmol/min/mg enzyme (*18*). A comparison of these values leads to the conclusion that if the content of propionyl-CoA dehydrogenase in *Salmonella typhimurium* or *Prototheca zopfii* is about 5% of the total protein in the extract, then the activity of pure propionyl-CoA dehydrogenase is at the same level as that of mammalian short-chain acyl-CoA dehydrogenases and *Megasphaera elsdenii* butyryl-CoA

dehydrogenase. However, because it is unlikely that a single enzyme accounts for 5% or more of the total protein, the activity of propionyl-CoA dehydrogenase is probably much higher than that of the mammalian and *Megasphaera elsdenii* dehydrogenases. It is desirable to investigate the molecular properties of purified propionyl-CoA dehydrogenases from propionate-oxidizing organisms: propionyl-CoA dehydrogenase may have a special mechanism to oxidize the substrate with a high standard redox potential.

In mammals, the reducing equivalents extracted from acyl-CoAs by acyl-CoA dehydrogenases are received by ubiquinone *via* two flavoproteins, electron-transferring flavoprotein and electron-transferring flavoprotein-ubiquinone oxidoreductase (*32*). Although a definitive value for the standard redox potential of ubiquinone in an aqueous environment has not been obtained, it has been estimated to be 70-110 mV (*22, 33*). The acrylyl-CoA/propionyl-CoA couple (69 mV) is very near to ubiquinone in its standard redox potential relative to longer enoyl-CoA/acyl-CoA couples (about −10 mV). This indicates the disadvantage of the oxidation of propionyl-CoA to acrylyl-CoA. Mammals metabolize propionyl-CoA mainly through the methylmalonyl-CoA pathway rather than β-oxidation. Succinate formed *via* the methylmalonyl-CoA pathway is then oxidized to fumarate and the extracted reducing equivalents are transferred to ubiquinone by succinate dehydrogenase. The standard redox potential of the fumarate/succinate couple is 31 mV (*22*), lower than that of the acrylyl-CoA/propionyl-CoA couple by about 40 mV, and consequently the oxidation of succinate to fumarate is thermodynamically more favorable than that of propionyl-CoA to acrylyl-CoA. At least in this point, the methylmalonyl-CoA pathway is more advantageous than the direct oxidation of propionyl-CoA to acrylyl-CoA.

Chemistry—To elucidate the physicochemical reason for the extraordinary standard redox potential of the C_3 couple, we used a semiempirical molecular orbital method (MOPAC). First, the reliability of the MOPAC calculation was examined. The dehydrogenation of alkane to alkene,

$$\text{alkane} \longrightarrow \text{alkene} + H_2,$$

is a simple model reaction for the dehydrogenation of acyl-CoA to enoyl-CoA. The ΔH (enthalpy change) of dehydrogenation can be obtained as the difference in the heat of formation (HOF) calculated by MOPAC ($HOF_{alkene} - HOF_{alkane}$). The following are lists of (name of alkene), (ΔH calculated by MOPAC) − (experimentally measured ΔH from literature (*34*)) = (difference between them) in kJ·mol^{-1}: acetylene, 145.6 − 137.3 = +8.3; propylene, 125.7 − 126.0 = −0.3; 1-butene, 129.1 − 126.9 = +2.2; 1-pentene, 129.1 − 126.0 = +3.1; 1-heptene, 129.1 − 126.0 = +3.1; *trans*-2-butene, 108.5 − 115.6 = −7.1; *trans*-2-pentene, 109.1 − 115.6 = −6.5. The MOPAC-calculated and measured values are in good agreement with each other. However, it should be noted that there may be differences between the calculated and measured values of up to ±10 kJ·mol^{-1}. Although the energy values that appear in the following discussion may contain small errors, the essence of the discussion is valid.

Figure 5 (upper) shows the MOPAC-calculated values of HOF of the acyl and enoyl forms of ethyl thioester. The CoA-S- moiety of the CoA-thioester was replaced by ethyl-S- for simplicity. The standard redox potential of a

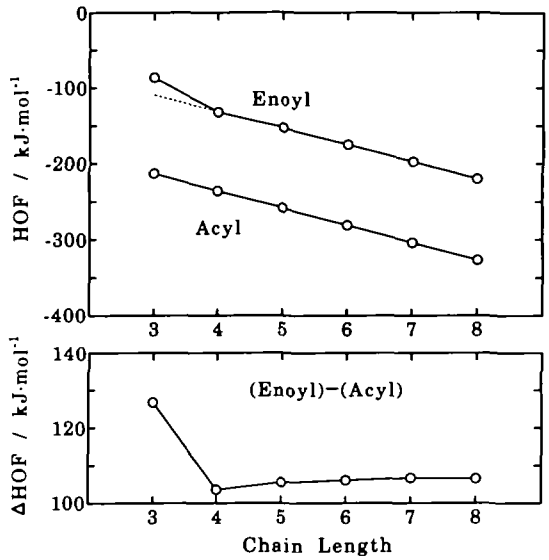

Fig. 5. **Calculated heat of formation (HOF) of acyl and enoyl forms of ethyl thioesters of different chain lengths.** Calculations were performed using a molecular orbital method (MOPAC). The lower panel shows the difference in HOF between the enoyl and acyl forms.

dehydrogenation system,

$$\text{Acyl} \longrightarrow \text{Enoyl} + H_2,$$

is represented as

$$E^{\circ\prime} = \frac{1}{2F}\Delta G^\circ + C = \frac{1}{2F}(\Delta H^\circ - T\Delta S^\circ) + C, \quad (5)$$

where ΔG°, ΔH°, and ΔS° are the standard Gibbs energy, standard enthalpy, and standard entropy of the dehydrogenation. C is a constant that depends on the experimental conditions, including pH, temperature, reference electrode, and so on. The standard enthalpy of dehydrogenation (ΔH°) can be calculated by $HOF_{enoyl} - HOF_{acyl}$ as described above, and the values are shown in Fig. 5 (lower). The ΔH° value for the C_3 couple is distinctly high while those for the C_4-C_8 couples are almost the same. This profile is consistent with the fact that the standard redox potential of the C_3 couple is extraordinarily higher than those of longer couples. The difference (23 kJ·mol^{-1}) in ΔH° between the C_3 and longer couples corresponds to the difference in the standard redox potential of 120 mV according to Eq. 5. That is, the actual difference in the standard redox potential (about 80 mV) between the C_3 couple and longer couples can be roughly explained by the enthalpy term.

The plots for the acyl forms in Fig. 5 are almost linear, that is, the increment in HOF by one methylene truncation is constant from C_8 to C_3. Similarly, the plots for the enoyl forms are also linear with the same slope as the acyl forms, except the value for C_3. The exceptionally high energy of the C_3-enoyl can be rationalized as follows. Upon ordinary one methylene truncation ($H\text{-}CH_2\text{-}CH_2\text{-}\!\!\rightarrow H\text{-}CH_2\text{-} + CH_2$), one C_{sp^3}-C_{sp^3} bond is eliminated. On the other hand, the one methylene truncation from C_4-enoyl to C_3-enoyl ($H\text{-}CH_2\text{-}CH=\!\!\rightarrow H\text{-}CH= + CH_2$) results in the elimination of one H-

C_{sp^3} and one C_{sp^3}-C_{sp^2} bond and the creation of one H-C_{sp^2} bond. This structural contrast must cause the energy change difference upon one methylene truncation because the bond energies differ between H-C_{sp^3} and H-C_{sp^2} and between C_{sp^3}-C_{sp^3} and C_{sp^3}-C_{sp^2}. A detailed energetic discussion is provided below.

The total energy (sum of the electronic energy and the inter-nucleic repulsion energy) calculated by MOPAC can be separated into a one-center energy for each atom and two-center energy for each pair of atoms (*35*). The two-center energy for a pair of atoms that form a direct bond with one another can be interpreted as corresponding to the bond energy, that is, a lower two-center energy represents a stabler or stronger bond between the pair of atoms. Figure 6 (upper two) shows the change in the two-center energies upon conversion from acyl to enoyl for C_3 and C_4. In both C_3 and C_4, the maximum change occurs at C(2)-C(3). [The numbering of the carbon atoms is as ····C(3)H=C(2)H-C(1)O-S-C_2H_5.] This is quite reasonable because the bonding between C(2) and C(3) changes from a single bond to a double bond, which should result in a very large change in bond energy. It is also shown that the two-center energies in which the C(2) and C(3) atoms participate are all lowered. This phenomenon can be ascribed to the change in the orbital hybridization of the C(2) and C(3) atoms from sp^3 to sp^2 upon the conversion from acyl to enoyl. It is known that an sp^2 hybridized orbital of a carbon atom

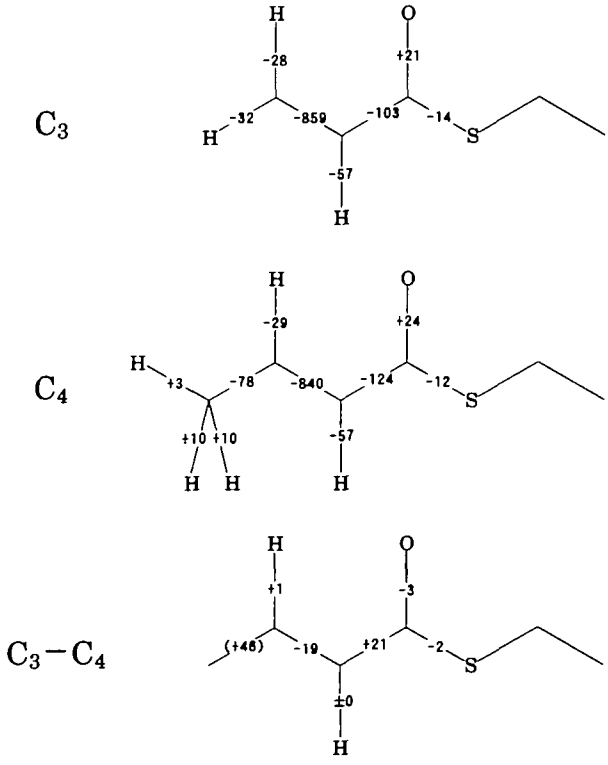

Fig. 6. **Changes in the two-center energies upon the conversion from acyl to enoyl.** The two-center energies were obtained by MOPAC calculation with the keyword ENPART. The label-free edges of line segments in the schemes represent carbon atoms. The values in the upper two schemes show the changes in the two-center energies upon the conversion from acyl to enoyl. Units are kJ·mol^{-1}. The lowest scheme shows the difference values between the upper schemes.

makes a stronger σ-bond than an sp^3 hybridized orbital because the larger contribution of the 2s orbital results in more expansion of the hybridized orbital and a larger overlap with the orbital of the partner atom (*36*). The degree by which the two-center energy is lowered depends on the partner atom: 28-57 kJ·mol^{-1} for hydrogen, 78 kJ·mol^{-1} for the carbon of the sp^3 orbital (C(4) of C_4), and 103-124 kJ·mol^{-1} for the carbon of the sp^2 orbital (C(2)), according to the calculated values shown in Fig. 6. The lowest scheme in Fig. 6 shows the difference in the values between the upper two schemes. The most essential difference between C_3 and C_4 is shown by the parenthesized value, which is caused by the difference in the atom that is connected to the C(3) atom. In other words, the energy for the C(3)-H bond changes by -32 kJ·mol^{-1} upon conversion from the C_3-acyl to C_3-enoyl, while the energy for the C(3)-C(4) bond changes by -78 kJ·mol^{-1} upon conversion from the C_4-acyl to C_4-enoyl. The difference between these changes ($+46$ kJ·mol^{-1}) contributes largely to the difference in $\Delta H^{\ddagger}$ between C_3 and C_4 (23 kJ·mol^{-1}); the residual -23 kJ·mol^{-1} is due to the sum of the other minor differences in the one-center and two-center energy changes. A scheme for one-center energies similar to Fig. 6 was also drawn (not shown). The values for the C_3-C_4 one-center energies (corresponding to the lowest scheme in Fig. 6) were all too small (absolute values less than 14 kJ·mol^{-1}) to be essential elements of the difference in $\Delta H^{\ddagger}$ between C_3 and C_4.

Other large values in the lowest scheme in Fig. 6 appear at C(1)-C(2) ($+21$ kJ·mol^{-1}) and C(2)-C(3) (-19 kJ·mol^{-1}). This tendency is consistent with the organic chemistry concept of hyperconjugation: in the C_4-enoyl, there is some contribution of the resonance structure, H_3C^+=CH-CH=(C-O$^-$)-S-. Anyway, the two values are complementary to each other so that together they have little effect. The one-center and two-center energies were also compared between C_4 and C_5. There were no significantly large values for C_4-C_5 in either the one-center or two-center energies (absolute values less than 7 kJ·mol^{-1}), supporting the proposal that there are no large structural differences between the C_4 and C_5 couple.

In conclusion, the extraordinarily higher standard redox potential of the C_3 couple compared with longer couples can be ascribed to the structure: the hydrogen atom is connected to the C(3) atom in the C_3 couple while the carbon atom is connected to the C(3) atom in C_4 and longer couples. The two-center energy of H-C(3) bonding is lowered by the acyl to enoyl conversion to a lesser extent than that of C(4)-C(3) bonding, and consequently the reduction of the C_3 couple is less favorable than the reduction of longer couples.

REFERENCES

1. Kunau, W.-H., Dommes, V., and Schulz, H. (1995) β-Oxidation of fatty acids in mitochondria, peroxisomes, and bacteria: a century of continued progress. *Prog. Lipid Res.* **34**, 267-342
2. Voet, D. and Voet, J. (1990) *Biochemistry*, Chapters 23 and 24, John Wiley & Sons, New York
3. Halarnkar, P.P. and Blomquist, G.J. (1989) Comparative aspect of propionate metabolism. *Comp. Biochem. Physiol.* **92B**, 227-231
4. Shaw, L. and Engel, P.C. (1984) The purification and properties of ox liver short-chain acyl-CoA dehydrogenase. *Biochem. J.* **218**, 511-520

5. Hauge, J.G. (1956) On the mechanism of dehydrogenation of fatty acyl derivatives of coenzyme A. IV. Kinetic studies. *J. Am. Chem. Soc.* **78**, 5266-5272
6. Stankovich, M.T. and Soltysik, S. (1987) Regulation of the butyryl-CoA dehydrogenase by substrate and product binding. *Biochemistry* **26**, 2627-2632
7. Lenn, N.D., Stankovich, M.T., and Liu, H. (1990) Regulation of the redox potential of general acyl-CoA dehydrogenase by substrate binding. *Biochemistry* **29**, 3709-3715
8. Cammack, R. (1995) Redox states and potentials in *Bioenergetics: A Practical Approach* (Brown, G.C. and Cooper C.E., eds.) pp. 85-109, Oxford University Press, Oxford
9. Kuchta, R.D. and Abeles, R.H. (1985) Lactate reduction in *Clostridium propionicum*. *J. Biol. Chem.* **260**, 13181-13189
10. Stadtman, E.R. (1957) Preparation and assay of acyl coenzyme A and other thiol esters: Use of hydroxylamine. *Methods Enzymol.* **3**, 931-941
11. Bernert, J.T. and Sprecher, H. (1977) An analysis of partial reactions in the overall chain elongation of saturated and unsaturated fatty acids by rat liver microsomes. *J. Biol. Chem.* **252**, 6736-6744
12. Williamson, G., Engel, P.C., Mizzer, J.P., Thorpe, C., and Massey, V. (1982) Evidence that the greening ligand in native butyryl-CoA dehydrogenase is a CoA persulfide. *J. Biol. Chem.* **257**, 4314-4320
13. Engel, P.C. (1981) Butyryl-CoA dehydrogenase from *Megasphaera elsdenii*. *Methods Enzymol.* **71**, 359-366
14. Ellison, P.A. and Engel, P.C. (1993) Intrinsic crotonase activity in a bacterial butyryl-CoA dehydrogenase. *Biochem. Mol. Biol. Int.* **29**, 605-612
15. Lau, S., Powell, P., Buettner, H., Ghisla, S., and Thorpe, C. (1986) Medium-chain acyl coenzyme A dehydrogenase from pig kidney has intrinsic enoyl coenzyme A hydratase activity. *Biochemistry* **25**, 4184-4189
16. Williamson, G. and Engel, P.C. (1982) A convenient and rapid method for the complete removal of CoA from butyryl-CoA dehydrogenase. *Biochim. Biophys. Acta* **706**, 245-248
17. Fink, C.W., Stankovich, M.T., and Soltysik, S. (1986) Oxidation-reduction potentials of butyryl-CoA dehydrogenase. *Biochemistry* **25**, 6637-6643
18. Williamson, G. and Engel, P.C. (1984) Butyryl-CoA dehydrogenase form *Megasphaera elsdenii*: Specificity of the catalytic reaction. *Biochem. J.* **218**, 521-529
19. Foust, G.P., Burleigh, B.D., Mayhew, S.G., Williams, C.H., and Massey, V. (1969) An anaerobic titration assembly for spectrophotometric use. *Anal. Biochem.* **27**, 530-535
20. Palmer, G. (1977) A versatile apparatus for performing anaerobic optical titrations with provision for multiple sampling of the reaction mixture. *Anal. Biochem.* **83**, 597-608
21. Dutton, P.L. (1978) Redox potentiometry: Determination of midpoint potentials of oxidation-reduction components of biological electron-transfer systems. *Methods Enzymol.* **54**, 411-435
22. Fasman, G.D. (1976) *Handbook of Biochemistry and Molecular Biology: Physical and Chemical Data*, 3rd ed., pp. 122-130, CRC Press, Boca Raton
23. Ikeda, Y., Dabrowski, C., and Tanaka, K. (1983) Separation and properties of five distinct acyl-CoA dehydrogenase from rat liver mitochondria. *J. Biol. Chem.* **258**, 1066-1076
24. Fernández-Briera, A. and Garrido-Pertierra, A. (1986) Determination of propionyl-CoA dehydrogenase activity in *Salmonella typhimurium* LT-2 cells by HPLC. *J. Liquid Chromatogr.* **9**, 2095-2109
25. Fernandez-Briera, A. and Garrido-Pertierra, A. (1988) A degradation pathway of propionate in *Salmonella typhimurium* LT-2. *Biochimie* **70**, 757-768
26. Wegener, W.S., Reeves, H.C., and Ajl, S.J. (1967) Propionate oxidation in *Escherichia coli*. *Arch. Biochem. Biophys.* **121**, 440-442
27. Kay, W.W. (1972) Genetic control of the metabolism of propionate by *Escherichia coli* K_{12}. *Biochim. Biophys. Acta* **264**, 508-521
28. Callely, A.G. and Lloyd, D. (1964) The metabolism of propionate in the colourless alga, *Prototheca zopfii*. *Biochem. J.* **92**, 338-345
29. Hodgson, B. and McGarry, J.D. (1968) A direct pathway for the conversion of propionate into pyruvate in *Moraxella lwoffi*. *Biochem. J.* **107**, 7-18
30. Hodgson, B. and McGarry, J.D. (1968) A direct pathway for the metabolism of propionate in cell extracts from *Moraxella lwoffi*. *Biochem. J.* **107**, 19-28
31. Shaw, L. and Engel, P.C. (1985) The suicide inactivation of ox liver short-chain acyl-CoA dehydrogenase by propionyl-CoA. *Biochem. J.* **230**, 723-731
32. Thorpe, C. (1991) Electron-transferring flavoprotein in *Chemistry and Biochemistry of Flavoenzymes* (Müller, F., ed.) Vol. 2, pp. 471-486, CRC Press, Boca Raton
33. Rich, P.R. (1984) Electron and proton transfers through quinones and cytochrome *bc* complexes. *Biochim. Biophys. Acta* **768**, 53-79
34. Morrison, R.T. and Boyd, R.N. (1987) *Organic Chemistry* 5th ed., pp. 297-342, Allyn and Bacon, Boston
35. Hirano, T. and Tanabe, K. (1998) *Bunshikidōhō MOPAC Gaidobukku* (in Japanese), Chapter 3, Kaibundo, Tokyo
36. McWeeny, R. (1979) *Coulson's VALENCE, Third Edition*, Chapter 7, Oxford University Press, Oxford